JOURNAL OF PROPULSION AND POWER
Vol. 15, No. 3, May–June 1999

Adaptive Control of Combustion Instability with On-Line System Identification

Shozo Koshigoe*
The Aerospace Corporation, Los Angeles, California 90009
Toshihiko Komatsuzaki†
California State University, Long Beach, California 90840-8305
and
Vigor Yang‡
Pennsylvania State University, University Park, Pennsylvania 16802

In this study, an adaptive control system is developed for suppressing pressure oscillations in a generic combustor, where the unsteady flowfield associated with the combustion instability is described by a nonlinear inhomogeneous wave equation. Control action is achieved by injecting auxiliary liquid fuel, and is modeled as an array of time-delayed combustion sources. The adaptive controller employs on-line system identification (SID) for robustness with respect to transient operating states, modeling uncertainties, external disturbances, and additional modes of instability that may arise in the course of control. Comparisons are made between the adaptive controller and a previously developed proportional-plus-integral (PI) controller, in terms of performance (degree of oscillation suppression, and speed with which oscillations are damped), robustness against plant parameter changes (particularly unknown factors of the auxiliary characteristics), and control-fuel mass expenditure. The adaptive controller exhibits good performance with a clear advantage over the PI controller in robustness. Also, the adaptive controller with on-line SID stabilizes the pressure oscillations without exciting additional mode(s).

Nomenclature

$\bar{a}$ = speed of sound in mixture
b_k = spatial distribution of burning rate of control fuel
$\bar{C}_v$ = constant volume specific heat for two-phase mixture
d = diameter of chamber
E_n^2 = Euclidean norm of nth acoustic mode
e = error signal between desired response and actual measurement
e_c = error signal for controller adaptation
e_{id} = error signal for SID adaptation
f = source term for boundary condition
h = noncontrol source term of wave equation
h_c = control source term of wave equation
K_D = derivative feedback gain
K_P = proportional feedback gain
k_n = wave number of nth acoustic mode
L = length of chamber
M = number of discrete combustion control sources
M_1 = length of $\boldsymbol{W}_{\mathrm{id}}^{(12)}$
$\dot{m}_{\mathrm{in}}$ = mass flow rate of control fuel
N = number of acoustic modes used in model
N_c = length of $\boldsymbol{W}_c$
N_1 = length of $\boldsymbol{W}_{\mathrm{id}}^{(11)}$
N_2 = length of $\boldsymbol{W}_{\mathrm{id}}^{(21)}$
$\boldsymbol{n}$ = unit outward normal vector
p = pressure
$\bar{p}$ = mean chamber pressure
$\tilde{p}_{\mathrm{in}}$ = output of SID model
p_{sen} = pressure sensor signal
$\bar{R}$ = gas constant for mixture
$\boldsymbol{r}$ = position vector
t = time
$\boldsymbol{u}$ = velocity
u_{in} = total acoustic pressure input produced by $\dot{m}_{\mathrm{in}}$
$\boldsymbol{W}_c$ = control parameter vector
$\boldsymbol{W}_{\mathrm{id}}^{(11)}$ = sensor part of SID parameter vector
$\boldsymbol{W}_{\mathrm{id}}^{(12)}$ = feedback part of SID parameter vector
$\boldsymbol{W}_{\mathrm{id}}^{(21)}$ = input part of SID parameter vector
$\bar{\gamma}$ = specific heat ratio for mixture
ΔH_c = heat of combustion of control fuel
δ = Dirac delta function with units, volume^{-1}
η_n = amplitude of nth mode
μ_c = gain constant for controller adaptation
μ_{id} = gain constant for SID adaptation
υ_c = time delay associated with controller
υ_k = time delay associated with kth control combustion source
ψ_n = normal mode function of nth mode
ω_n = normal frequency of nth mode

Subscripts

c = controller
dc = constant component
id = system identification
sen = sensor

Superscripts

$'$ = fluctuation
$-$ = mean
$\cdot$ = time derivative

Received July 11, 1997; revision received Sept. 6, 1998; accepted for publication Sept. 14, 1998.

*Member of Technical Staff.
†M.S. Student, Department of Mechanical Engineering.
‡Professor, Department of Mechanical Engineering, 106 Research Building East. Associate Fellow AIAA.

I. Introduction

THE goal of actively controlling combustion instability has received growing emphasis as a result of improvements in modern control hardware and algorithms, as well as more stringent system demands (such as reduced vibration tolerances in rocket motors, or lower emission level requirements for gas-turbine

engines). Adaptive control has demonstrated success in the related field of active noise/vibration control,[1] and offers important advantages over state-of-the-art fixed-parameter control of combustion instability.[2–4] When combined with on-line system identification, the adaptive approaches can be especially robust in the face of transient operating states, modeling uncertainties, external disturbances, and additional modes of instability that may arise as a result of the control actions. Concerning the combustion control hardware, various actuation schemes have been proposed, including acoustic forcing,[5–9] e.g., loudspeakers, periodic heat removal by controlled water injection, excitation of reactive shear layers,[10–12] and regulation of mass flow rate through the combustor.[13] The most promising actuation appears to be controlled modulation of the fuel flow[14–16] (primary or auxiliary), because the high-energy density of the control fuel makes feasible the extension to full-scale combustors. References 17–19 provide more detailed reviews of the status of active combustion control algorithms and hardware.

Although nearly all preceding active control schemes for combustion instability have used fixed-parameter controllers, adaptive approaches may be practically essential to address the issues of transient operating states, modeling uncertainties, additional modes of instability that may arise, and external disturbances (such as noise). An adaptive strategy was employed in Ref. 12, but the controller parameters were adjusted by direct minimization of the performance cost function. System identification (SID) can offer improvements over direct adaptation by utilizing information of the system dynamics to allow more intelligent updating of the control parameters. The adaptive controller of Ref. 15 used off-line SID, in which the I/O frequency responses of the SID model and the actual combustor were matched to determine the model coefficients. Then, the model parameters were fixed for incorporation into the adaptive controller. Under certain conditions, in controlling the dominant mode(s) of instability, the controller appeared to excite another mode, although its amplitude did not grow large. Perhaps on-line SID could avoid this problem by providing a continuously updated model of the system dynamics, in the simultaneous presence of controller actions. Furthermore, on-line SID eliminates the need for a separate SID procedure before the controller can be activated. Whether or not SID is utilized, the additional issues of stability and convergence for an adaptive controller should also be addressed for successful implementation into actual systems.

The methodology presented in this paper uses controlled injection of auxiliary fuel, with an adaptive controller employing on-line SID for rapid and accurate optimization of the control action with enhanced robustness. An analytical framework developed in Refs. 2–4 is used to treat the auxiliary fuel combustion as well as the entire oscillatory flowfield in a generic combustor. The adaptive controller is based on work done in the field of noise/vibration control, specifically on the problem of suppressing payload fairing internal noise. Active noise-control technology was first applied to this problem in Refs. 20 and 21, using a simplified fairing model consisting of an elastic plate backed by a rigid cavity. That controller has been successfully upgraded to an adaptive controller with on-line SID,[1] similar to the one developed here for controlling combustion instabilities. Additionally, an established proportional-plus-integral (PI) fixed parameter controller[2–4] is used for baseline comparisons. The focus in this paper will be on controlling longitudinal instabilities in a solid rocket motor, but application to other acoustic-coupled modes and other types of combustors is feasible.

II. Formulation

The system under consideration is given in Fig. 1. Pressure signals from the combustor are fed to the SID and control unit, which determines the appropriate control commands for the auxiliary fuel injector. The injected fuel then undergoes a distributed combustion process to generate the excitations required to modulate the unsteady motions within the combustor. The model describing the oscillatory flowfield follows that of Fung et al.[2] and Fung and Yang,[4] which is based on the two-phase formulation established by Culick and Yang.[22] The basic idea is to formulate the conservation equations for a single-phase medium into which the effects of the liquid

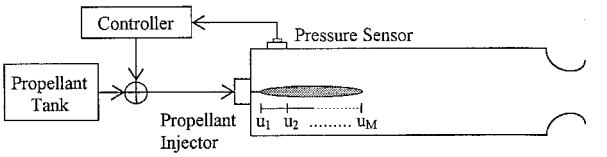

Fig. 1 Schematic diagram of solid rocket motor and control system with distributed actuators.

phase can be incorporated. With the use of a perturbation expansion method, where the dependent variables are decomposed as sums of mean and fluctuating components, the following wave equation is derived for the unsteady motions in the combustor:

$$\nabla^2 p' - \frac{1}{\bar{a}^2}\frac{\partial^2 p'}{\partial t^2} = h + h_c \tag{1}$$

with boundary conditions

$$\boldsymbol{n}\cdot\nabla p' = -f \tag{2}$$

The source terms h and f include all of the influences of the primary fuel combustion (not including the combustion of the auxiliary fuel), mean flow, nonlinear gasdynamics, surface admittances, etc., and are defined in Ref. 22 along with the mean speed of sound, $\bar{a}$. The source term h_c represents the influence arising from the combustion of the auxiliary fuel. With a knowledge of the mean flowfield and injector characteristics, and assuming that the combustion response of the injected fuel depends primarily on the local fluctuations in pressure and velocity, h_c can be expressed as a function of the control actions and the flow oscillations. The details of how unsteady flow motions affect combustion and vice versa, are in some ways the most essential, yet least understood aspects of the general combustion instability problem. The physicochemical processes involved can vary widely among different combustion systems, and may entail complicated dynamics involving flame stretching, fuel droplet atomization, turbulent enhancement of transport properties, gaseous-condensed phase interactions, etc. Here, the spatial distribution of the controlled heat release is approximated as an array of M discrete sources, and the generalized time-lag theory of Crocco and Cheng[23] is used to model the progress of the control fuel from injection to complete combustion. The auxiliary fuel source term, h_c, then can be written

$$h_c = -\frac{\bar{R}\Delta\, H_c}{\bar{a}^2\bar{C}_v}\sum_{k=1}^{M}\frac{\partial \dot{m}_{\text{in}}(t-\tau_k)}{\partial t}b_k\delta(\boldsymbol{r}-\boldsymbol{r}_k) \tag{3}$$

The time delay, τ_k, is the time at which an element of fuel burns at the kth combustion source, measured from the moment of its injection. The spatial distribution parameter, b_k, measures the fraction of control fuel currently burning within the volume represented by the kth combustion source, located at $\boldsymbol{r}_k$. Conservation of mass requires that

$$\sum_{k=1}^{M} b_k = 1$$

To solve Eq. (1), an approximate technique based on the Galerkin method is employed, in which the fluctuating pressure and velocity fields are expressed as series of the acoustic normal modes with time varying coefficients $\eta_n(t)$:

$$p'(\boldsymbol{r},t) = \bar{p}\sum_{n=1}^{\infty}\eta_n(t)\psi_n(\boldsymbol{r}), \qquad \boldsymbol{u}'(\boldsymbol{r},t) = \sum_{n=1}^{\infty}\frac{\dot{\eta}_n(t)}{\bar{\gamma}k_n^2}\nabla\psi_n(\boldsymbol{r}) \tag{4}$$

Here ψ_n is the nth acoustic normal mode, which is an eigenfunction solution to Eqs. (1) and (2), after assuming time-harmonic behavior and setting all of the source terms equal to zero. By substituting Eq. (4) into Eq. (1), and applying the Galerkin method using the

normal modes as weighting functions, the following system of dynamical equations is found for the time evolution of each mode:

$$\ddot{\eta}_n + \omega_n^2 \eta_n = \frac{\bar{a}^2}{\bar{p} E_n^2} \sum_{k=1}^{M} [b_k u_{\text{in}}(t - \upsilon_k)] \psi_n(\boldsymbol{r}_k)$$

$$- \sum_{i=1}^{N} \{D_{ni} \dot{\eta}_i + E_{ni} \eta_i\} - \sum_{i=1}^{N} \sum_{j=1}^{N} \{A_{nij} \dot{\eta}_i \dot{\eta}_j + B_{nij} \eta_i \eta_j\} \quad (5)$$

The coefficients D_{ni} and E_{ni} represent all linear processes in h and f, and A_{nij} and B_{nij} arise from the nonlinear gasdynamic processes; these coefficients are defined in Ref. 22. The function, $u_{\text{in}}(t - \upsilon_k)$, represents the actuation of the kth control combustion source, and is related to the controlled fuel flow rate as follows:

$$u_{\text{in}}(t - \upsilon_k) = \frac{\bar{R}\Delta\, H_c}{\bar{a}^2 \bar{C}_v} \frac{\partial \dot{m}_{\text{in}}(t - \upsilon_k)}{\partial t} \quad (6)$$

In Fig. 1, the control input to the system from each of the discrete combustion sources is represented as $u_1, u_2, \ldots, u_M$. These individual inputs are not independent of each other, nor do they explicitly appear in the control algorithm. The only quantity that the controller actually controls is the flow of fuel through the auxiliary injector. However, this single controlled quantity is manifested as the M discrete control combustion sources according to the model outlined earlier.

III. Controller Algorithms

The purpose of the controller is to determine an appropriate $u_{\text{in}}(t - \upsilon_k)$ for suppressing the combustion instability, based on information provided by the sensor. Many well-developed theories exist for the synthesis and optimization of fixed-parameter controllers, and the resulting designs are usually simpler and cheaper to implement than their adaptive counterparts. However, transient operating states and uncertain or incomplete models are typically encountered for combustion control problems, as well as unpredictable disturbances (such as noise), and other modes of instability that may arise in the course of control. Under such off-design circumstances, fixed parameter controllers will generally suffer decreased performance at best, and complete failure at worst. Adaptive controllers, with the ability to automatically adjust themselves to the situation at hand, can offer acceptable performance over a range of operating conditions in the presence of modeling uncertainties/inadequacies, external disturbances, and additional modes of instability that may arise. In some combustion control applications, adaptive approaches may be the only viable alternative. An adaptive controller is studied here with a fixed parameter controller[2–4] considered as a baseline for comparison.

In controlling combustion instability, it would be advantageous to have an actuator that could both add and subtract heat from the flowfield according to the prespecified requirements. The Rayleigh criterion provides that acoustic waves are damped if heat is added during the rarefaction phase of the local pressure fluctuations, or if heat is removed during the compression phase. At a single point in space, Rayleigh's criterion can be expressed mathematically in terms of the time-integrated product of the local pressure fluctuation and heat release fluctuation, $\dot{q}'$, as follows:

$$\int_T p' \dot{q}' \, \mathrm{d}t \quad (7)$$

Here, T is the period of the pressure oscillations. If this integral is positive/negative, the unsteady heat release at the given point tends to drive/damp the instability. Notice that it is the fluctuation of heat release that is the quantity of interest. Although combustion of the auxiliary fuel is always an exothermic process, a negative $\dot{q}'$ is viewed by the instability as a removal of heat relative to the mean heat release. This is practically realized by allowing for a constant component in the auxiliary injector fuel flow:

$$\dot{m}_{\text{in}} = \dot{m}_{\text{in},dc} + \int_0^t \dot{m}_{\text{in}} \, \mathrm{d}t' = \dot{m}_{\text{in},dc} + \frac{\bar{a}^2 \bar{C}_v}{\bar{R}\Delta\, H_c} \int_0^t u_{\text{in}}(t') \, \mathrm{d}t' \quad (8)$$

Here, $\dot{m}_{\text{in},dc}$ is the unmodulated mass flow rate. By decreasing the mass flow of auxiliary fuel below $\dot{m}_{\text{in},dc}$, the controller can effectively remove heat, relative to the mean flow conditions. Of course, the maximum amount of heat removal would be limited by the size of $\dot{m}_{\text{in},dc}$, because the injector cannot physically have a negative mass flow rate. Any control signal calling for negative mass flow rate would therefore be clipped at zero; hence, increasing $\dot{m}_{\text{in},dc}$ increases the clipping margin.

Following Refs. 2–4, a proportional-plus-integral scheme is used for the fixed parameter controller. Because it is the time derivative of the fuel injection rate that exerts direct influence on the oscillatory flowfield, the PI control law is equivalent to introducing proportional-plus-derivative (PD) control action:

$$u_{\text{in}}(t) = \frac{\bar{R}\Delta\, H_c}{\bar{a}^2 \bar{C}_v} \left[\frac{\partial \dot{m}_{\text{in}}(t)}{\partial t} \right] = K_P e(t - \upsilon_c) + K_D \dot{e}(t - \upsilon_c) \quad (9)$$

where $e(t)$ is the error signal between the desired system response and the measured pressure fluctuation. In this study, the chamber oscillations are monitored by a point sensor located at position $\boldsymbol{r}_s$, with output p_{sen}. The controller time lag, υ_c, is the actual time required for data acquisition, signal processing, and dynamic response of the fuel-injection mechanism. Because this time lag applies uniformly to all M control combustion sources, it can be simply absorbed into the time lag of each source, υ_k. The methodology for choosing K_P and K_D to minimize controller sensitivity to variations in actuator time delay, and to minimize control input energy, is detailed in Refs. 2 and 4.

The actuation for the adaptive controller can be specified as

$$u_{\text{in}}(t) = \bar{p} Ctrl(t - \upsilon_c) \quad (10)$$

As before, the controller time lag can be absorbed into the υ_k. In reality, the adaptive controller would employ digital filters and discrete-time signal processing, and so the following digital expression for $Ctrl$ is used:

$$Ctrl(i) = \sum_{j=0}^{N_c} [W_c(i)]_j \, p_{\text{sen}}(i - j) \quad (11)$$

where $Ctrl(i)$ and $p_{\text{sen}}(i)$ are the control signal and sensor signal, respectively, at the ith discretized time step. The control parameters $[W_c(i)]_j$, for the ith time step, are contained in the vector $\boldsymbol{W}_c(i)$ of length N_c, and determine how the sensor measurement is used to generate the control action. For example, limiting $\boldsymbol{W}_c(i)$ to a single element ($N_c = 1$), and setting $[W_c(i)]_1 = K_P/\bar{p}$, the adaptive controller would basically serve as a digital proportional controller, i.e., a digital version of the PI controller with $K_D = 0$ in Eq. (9). Lengthening $\boldsymbol{W}_c$ effectively allows higher-order derivative- and/or integral-type control laws. Furthermore, the adaptive controller allows the elements of $\boldsymbol{W}_c$ to be changed at each time step. Determining an appropriate updating scheme for these control parameters is the essential task in this adaptive control problem.

In this study, on-line SID is used in determining control parameters $\boldsymbol{W}_c$, which yield suppression of the combustion instability. The basic idea is to maintain a simplified generic model of the controlled system, from which information can be derived for intelligent updating of the control parameters. The SID model employed here has the following form:

$$\tilde{p}_{\text{in}}(i) = Y_1(i) + Y_2(i) \quad (12)$$

where $\tilde{p}_{\text{in}}(i)$ is the SID model output at the ith time step. The digital filter Y_1 has p_{sen} as input, and includes the feedback term, and Y_2 has the control signal as input:

$$Y_1(i) = \sum_{j=0}^{N_1} \left[W_{\text{id}}^{(11)}(i) \right]_j p_{\text{sen}}(i - j)$$

$$+ \sum_{j=0}^{M_1} \left[W_{\text{id}}^{(12)}(i) \right]_j \tilde{p}_{\text{in}}(i - j - 1) \quad (13)$$

$$Y_2(i) = \sum_{j=0}^{N_2} \left[W_{\mathrm{id}}^{(21)}(i)\right]_j Ctrl(i-j) \tag{14}$$

The SID parameters are contained in the vector $\boldsymbol{W}_{\mathrm{id}}(i)$, which is split into three parts: $\boldsymbol{W}_{\mathrm{id}}^{(11)}(i)$, $\boldsymbol{W}_{\mathrm{id}}^{(12)}(i)$, and $\boldsymbol{W}_{\mathrm{id}}^{(21)}(i)$ of lengths N_1, M_1, and N_2, respectively. The SID parameters are adjusted at each time step to minimize the SID error, defined as

$$e_{\mathrm{id}}^2(i) = \tfrac{1}{2}[p_{\mathrm{sen}}(i) - \tilde{p}_{\mathrm{in}}(i)]^2 \tag{15}$$

If the preceding quantity is kept small, that means the SID model has converged and is accurately reproducing the behavior of the combustion system. However, because Eq. (11) can hardly be expected to comprehensively represent the physics of the problem, the converged model is likely to be valid only over a short period of time. Furthermore, changing operating conditions would also eventually make a converged model obsolete. Therefore, the SID model parameters are updated at each time step as follows, to keep the model currently accurate (albeit only locally valid).

$$\boldsymbol{W}_{\mathrm{id}}^{(11)}(i+1) = \boldsymbol{W}_{\mathrm{id}}^{(11)}(i) - \mu_{\mathrm{id}} \nabla_{\mathrm{id}}^{(11)} e_{\mathrm{id}}^2(i) \tag{16}$$

$$\boldsymbol{W}_{\mathrm{id}}^{(12)}(i+1) = \boldsymbol{W}_{\mathrm{id}}^{(12)}(i) - \mu_{\mathrm{id}} \nabla_{\mathrm{id}}^{(12)} e_{\mathrm{id}}^2(i) \tag{17}$$

$$\boldsymbol{W}_{\mathrm{id}}^{(21)}(i+1) = \boldsymbol{W}_{\mathrm{id}}^{(21)}(i) - \mu_{\mathrm{id}} \nabla_{\mathrm{id}}^{(21)} e_{\mathrm{id}}^2(i) \tag{18}$$

This updating scheme is based on the least-mean-square (LMS) algorithm described in Ref. 24. The gain constant, μ_{id}, is chosen large enough to allow rapid convergence of the system identification, yet small enough to ensure stability of the algorithm. The operator, $\nabla_{\mathrm{id}}^{(nm)}$, is the gradient taken with respect to the elements of the (nm) part of the SID parameter vector. Specifically, the jth element of each of the last vector terms in the preceding equations are, respectively,

$$\left[\nabla^{(11)} e_{\mathrm{id}}^2(i)\right]_j = e_{\mathrm{id}}(i) \frac{\partial e_{\mathrm{id}}(i)}{\partial \left[W_{\mathrm{id}}^{(11)}(i)\right]_j}$$

$$= -[p_{\mathrm{sen}}(i) - \tilde{p}_{\mathrm{in}}(i)] p_{\mathrm{sen}}(i-j) \tag{19}$$

$$\left[\nabla^{(12)} e_{\mathrm{id}}^2(i)\right]_j = e_{\mathrm{id}}(i) \frac{\partial e_{\mathrm{id}}(i)}{\partial \left[W_{\mathrm{id}}^{(12)}(i)\right]_j}$$

$$= -[p_{\mathrm{sen}}(i) - \tilde{p}_{\mathrm{in}}(i)] \tilde{p}_{\mathrm{in}}(i-j-1) \tag{20}$$

$$\left[\nabla^{(21)} e_{\mathrm{id}}^2(i)\right]_j = e_{\mathrm{id}}(i) \frac{\partial e_{\mathrm{id}}(i)}{\partial \left[W_{\mathrm{id}}^{(21)}(i)\right]_j}$$

$$= -[p_{\mathrm{sen}}(i) - \tilde{p}_{\mathrm{in}}(i)] Ctrl(i-j) \tag{21}$$

To use the on-line SID to update the controller parameters, the controller error at the ith time step is first defined:

$$e_c^2(i) = \tfrac{1}{2}[\tilde{p}_{\mathrm{in}}(i)]^2 \tag{22}$$

We wish to damp out the oscillations within the chamber, which corresponds to minimizing $e_c^2(i)$ for converged SID. The following LMS-based updating is therefore used for the control parameters:

$$\boldsymbol{W}_c(i+1) = \boldsymbol{W}_c(i) - \mu_c \nabla_c e_c^2(i) \tag{23}$$

where

$$\left[\nabla_c e_c^2(i)\right]_j = e_c(i) \frac{\partial e_c(i)}{\partial [W_c(i)]_j}$$

$$= \tilde{p}_{\mathrm{in}}(i) \sum_{j=0}^{N_2} \left[W_{\mathrm{id}}^{(21)}(i)\right]_j p_{\mathrm{sen}}(i-k-j) \tag{24}$$

Therefore, the information concerning combustor behavior gained from the SID model has been used to adjust the control parameters. Specifically, $\tilde{p}_{\mathrm{in}}$ and $\boldsymbol{W}_{\mathrm{id}}^{(21)}$ enter into the update law. The gain constant, μ_c, determines the convergence speed and stability of this updating. The overall structure of the entire adaptive controller is given schematically in Fig. 2.

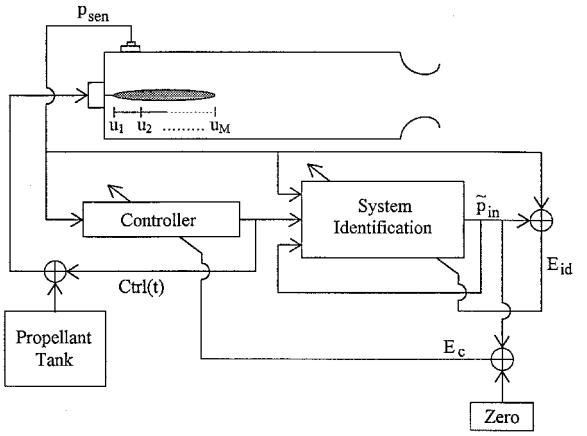

Fig. 2 Adaptive controller with on-line system identification.

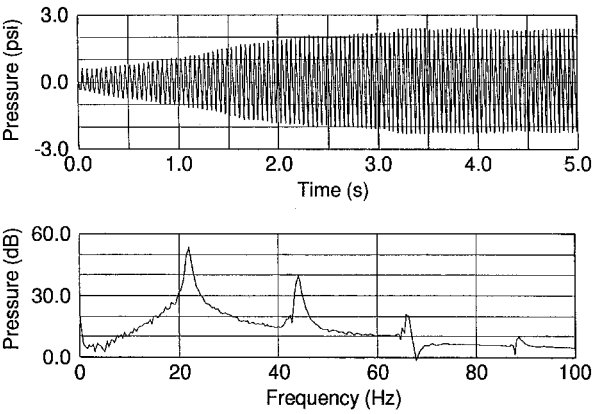

Fig. 3 Pressure oscillations at chamber head end as a function of time and frequency.

IV. Discussion of Results

The adaptive control system is exercised on a model problem, in which oscillations in a solid booster rocket motor are controlled using monomethylhydrazine (MMH) as the auxiliary fuel. The model parameters for the combustion chamber used here are shown next. $\bar{a} = 1270$ m/s, $\bar{p} = 4.83$ MPa, $L = 33$ m, $d = 1.7$ m, $\bar{\gamma} = 1.2$, $\bar{R} = 378$ J/kg/K, $\bar{C}_v = 1571$ J/kg/K, and $\Delta H_c = 28.3 \times 10^6$ J/kg. These numbers are representative of a large solid rocket motor, for which longitudinal combustion instabilities are the most common modes. To make the simulation more representative of realistic combustor performance, modal frequency shift (each mode frequency was changed by 20% of its original value) and stochastic behavior are included in the simulation. An example of uncontrolled behavior is given in Fig. 3. The pressure-time trace at the head of the chamber is for an initial disturbance of 0.5 psi, which grows and reaches a limit cycle with an amplitude of about 3% of the mean pressure. The frequency spectrum clearly shows the existence of the first (22 Hz) and higher modes.

For the PI controller, Fig. 4 presents the contours of normalized energy of the pressure oscillation as a function of the derivative gain, K_D, and the injection time delay, τ_{norm} (normalized by the period of the fundamental mode). The normalized energy is calculated by using Eqs. (2), (5), and (6). The solid white portions of Fig. 4 represent regions where the PI controller is unable to suppress the instability; therefore, the controller is not stable when the time delay equals approximately half the period of the fundamental mode. For any time delay, K_D exist that make the controller unstable, and so the PI controller is not robust with respect to changes in time delay or K_D. Also for the PI controller, Fig. 5 shows the contours of total

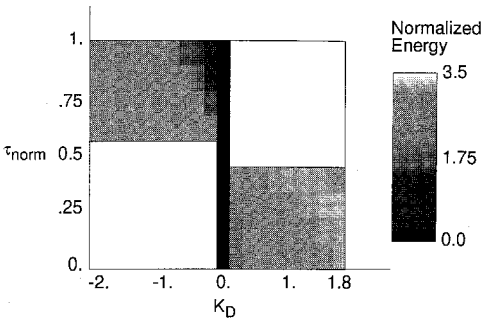

Fig. 4 Normalized energy of controlled oscillations as a function of normalized injector time delay and PI control parameter, K_D.

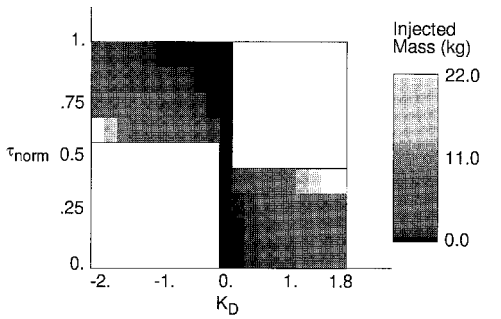

Fig. 5 Total mass of control fuel used over 5 s of control action as a function of injector time delay and PI control parameter, K_D.

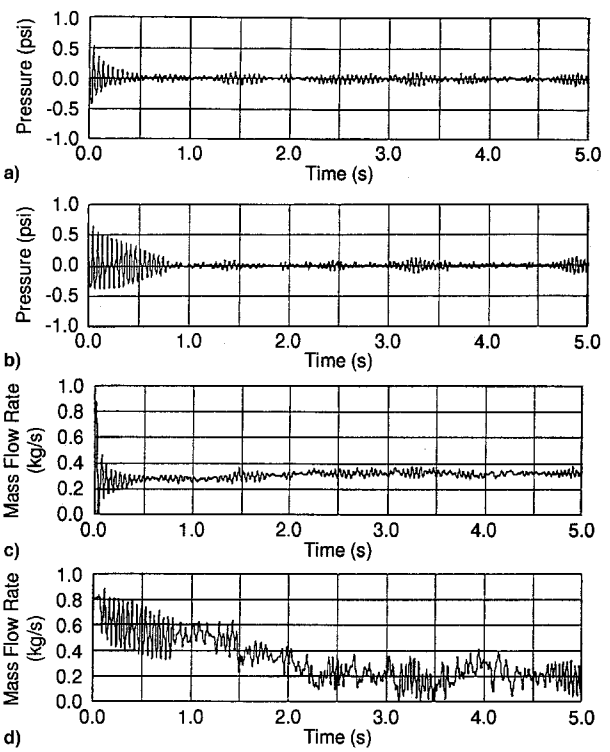

Fig. 6 Comparison of controlled pressure time traces for injection time delay, $\tau_{\text{norm}} = 0.9$ and PI control parameter, $K_D = -1.4$, using a) PI controller; b) adaptive controller; and the corresponding $\dot{m}$ traces, c) and d), respectively.

injected control fuel over 5 s of control simulation for different values of υ_{norm} and K_D. The total amount of fuel used for control is an important practical concern, especially for systems like the current one, which has stringent volume or weight limitations.

A comparison between performance of the adaptive and PI controllers is made in Fig. 6. The control parameter, $K_D = -1.4$, and the injection time delay, $\upsilon_{\text{norm}} = 0.9$, are chosen so that the PI controller shows good control performance with reasonably small control fuel consumption. Both controlled pressure-time traces exhibit rapid suppression of the pressure oscillation, with the PI controller reducing the initial disturbance to within the noise level in about 0.5 s, and the adaptive controller damping the disturbance in about 0.75 s. The corresponding mass flow rates are given as functions of time. These results are obtained by assuming a value of $\dot{m}_{\text{in},dc}$ large enough so that there is no clipping of the mass flow rate. The adaptive controller appears to use significantly more control fuel in the initial damping period. Once the combustor has been stabilized, both controllers maintain similarly low oscillation amplitudes, but noticeable modulation of the control fuel still occurs, probably as a result of the stochastic disturbances. During the stabilized period, e.g., for times past 1 s, these oscillations in auxiliary fuel flow have peak-to-peak variations within about 0.1 kg/s for the PI control, and within about 0.4 kg/s for the adaptive control, which is nearly enough to clip the control fuel flow at some points. For times after 2 s, the local time-averaged flow rate of the control fuel appears to stay slightly above 0.3 kg/s for the PI controller, but is generally lower for the adaptive controller, around 0.2 kg/s. So

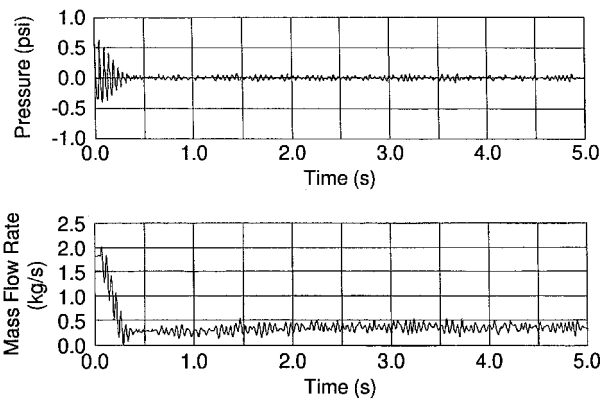

Fig. 7 Controlled pressure time trace and corresponding $\dot{m}$ time trace for adaptive controller, with injector time delay $\tau_{\text{norm}} = 0.5$.

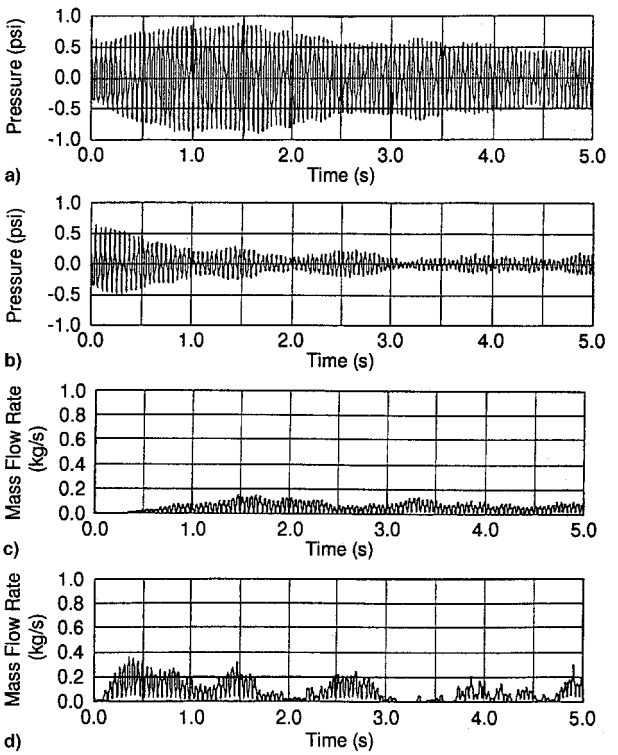

Fig. 8 Comparison of controlled pressure for $\dot{m}_{\text{in},dc} = 0$ with $\tau_{\text{norm}} = 0.9$ and $K_D = 1.4$, using a) PI controller; b) adaptive controller; and corresponding $\dot{m}$ time traces, c) and d), respectively.

based on the 5 s of control history shown in Fig. 6, the adaptive controller expends more fuel to initially control the instability, but uses less fuel in maintaining stability, once the combustor has been controlled. Ideally, the system would spend all of its time in a controlled state, making the adaptive controller more fuel efficient in the long run.

The robustness of the adaptive controller has been tested with respect to several different injection time delays, and was found to be stable in all cases. Figure 7 shows the controlled pressure trace and the corresponding control fuel mass flow-rate trace of the adaptive controller with $\tau_{\text{horm}} = 0.5$. The PI controller is unstable for this time delay. The adaptive controller clearly demonstrates its advantage over the PI controller for robustness in terms of injector uncertainty (represented by uncertainty in the time delay). Comparing Figs. 6 and 7, for $\tau_{\text{horm}} = 0.5$ the adaptive controller shows faster damping of the initial disturbance than the PI controller with $K_D = -1.4$ and $\tau_{\text{horm}} = 0.9$, or the adaptive controller with $\tau_{\text{horm}} = 0.9$.

Robustness of the two controllers is also examined with respect to clipping of the control fuel flow rate. In Fig. 8, $\tau_{\text{horm}} = 0.9$, and the unmodulated mass flow rate, $\dot{m}_{\text{in},dc} = 0$, is chosen so that roughly half of the modulated mass flow rate is clipped. The PI controller exerts very limited influence on the unsteady motions, with substantial persisting oscillations. The adaptive controller, however, keeps the oscillations at a significantly lower amplitude, illustrating superior robustness of the adaptive controller with respect to the control fuel flow clipping.

Figure 9 compares the PI and adaptive controllers on the bases of control fuel consumption and pressure oscillation suppression vs unmodulated control fuel flow. The total injected control fuel mass and normalized energy of the pressure oscillations are plotted as functions of the unmodulated mass flow rate, $\dot{m}_{\text{in},dc}$ for both the PI and adaptive controllers with time delay $\tau_{\text{horm}} = 0.9$. The plots show that the adaptive controller uses slightly more total control fuel than the PI controller, especially for higher values of $\dot{m}_{\text{in},dc}$, where there is no clipping (above 1 kg/s, approximately). However, the adaptive controller shows definite performance advantage over the PI controller for smaller values of $\dot{m}_{\text{in},dc}$, where clipping occurs.

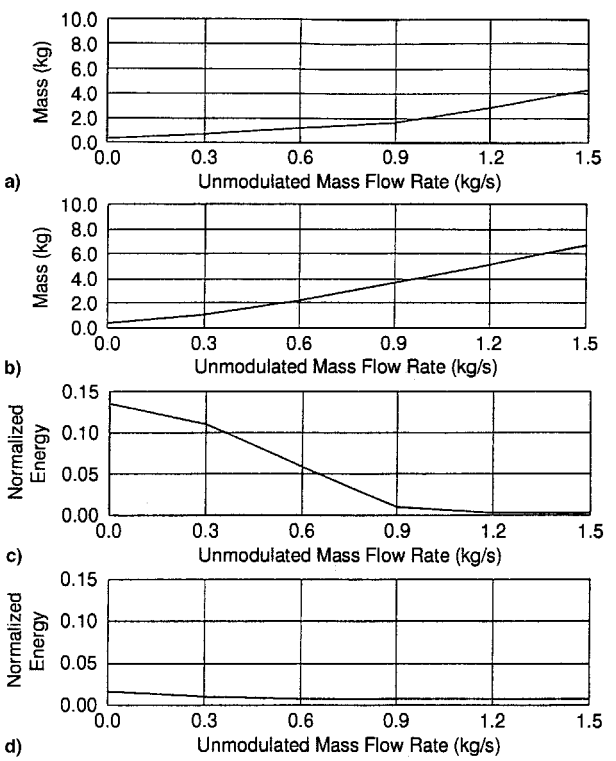

Fig. 9 Comparison of total injected fuel mass vs $\dot{m}_{\text{in},dc}$ using a) PI controller; and b) adaptive controller for the injection delay $\tau_{\text{norm}} = 0.9$; and normalized energy vs $\dot{m}_{\text{in},dc}$, c) and d), respectively.

V. Conclusions

In this study, an adaptive control system utilizing on-line system identification is developed for suppressing combustion instabilities in a generic combustor. Pressure oscillations are described by a nonlinear inhomogeneous wave equation. The control system consists of a pressure sensor, the controller, and a fuel injector, with the control fuel combustion represented by an array of time delayed distributed combustion sources. To test the control strategy, simulations are conducted for control of combustion instabilities in a large solid-propellant rocket motor. The controller performance is examined in terms of robustness against plant parameter changes (especially unknown factors concerning control injector performance), pressure oscillation suppression speed, and control fuel mass consumption. The adaptive controller is compared with a fixed parameter (PI) controller, showing that the adaptive controller is more robust with respect to system uncertainty. Specifically, the adaptive controller demonstrated acceptable performance over a range of injection time delay and unmodulated control fuel flow, whereas the fixed parameter controller did not. For optimal conditions, the PI controller may exhibit somewhat better performance than the adaptive system; however, the robustness advantages of the adaptive controller definitely make it a more attractive choice for practical applications. Additionally, in all cases considered, the adaptive controller with on-line system identification suppressed the dominant modes of instability without exciting another mode(s).

References

[1]Koshigoe, S., Teagle, A., Tsay, C. H., Morishita, S., and Une, S., "Numerical Simulation of Active Control with On-Line System Identification on Sound Transmission Through an Elastic Plate," *Journal of the Acoustical Society of America*, Vol. 99, No. 5, 1996, pp. 2947–2954.

[2]Fung, Y.-T., Yang, V., and Sinha, A., "Active Control of Combustion Instabilities with Distributed Actuators," *Combustion Science and Technology*, Vol. 78, No. 4–6, 1991, pp. 217–245.

[3]Yang, V., Sinha, A., and Fung, Y.-T., "State-Feedback Control of Longitudinal Combustion Instabilities," *Journal of Propulsion and Power*, Vol. 8, No. 1, 1992, pp. 66–73.

[4]Fung, Y.-T., and Yang, V., "Active Control of Nonlinear Pressure Oscillations in Combustion Chambers," *Journal of Propulsion and Power*, Vol. 8, No. 6, 1992, pp. 1282–1289.

[5]Dine, P. J., "Active Control of Flame Noises," Ph.D. Dissertation, Cambridge Univ., Cambridge, England, UK, 1983.

[6]Heckl, M. A., "Active Control of the Noise from a Rijke Tube," *IUTAM Symposium on Aero- and Hydro-Acoustics, Lyon 1985*, Springer–Verlag, Berlin, 1986, pp. 211–216.

[7]Lang, W., Poinsot, T., and Candel, S., "Active Control of Combustion Instability," *Combustion and Flame*, Vol. 70, No. 3, 1987, pp. 281–289.

[8]Poinsot, T., Bourienne, F., Candel, S., Esposito, E., and Lang, W., "Suppression of Combustion Instabilities by Active Control," *Journal of Propulsion and Power*, Vol. 5, No. 1, 1987, pp. 14–20.

[9]Gulati, A., and Mani, R., "Active Control of Unsteady Combustion-Induced Oscillations," *Journal of Propulsion and Power*, Vol. 8, No. 5, 1992, pp. 1109–1115.

[10]Gutmark, E., Parr, T. P., Wilson, K. J., Hanson-Parr, D. M., and Schadow, K. C., "Closed-Loop Control in a Flame and a Dump Combustor," *IEEE Control Systems*, Vol. 13, No. 1, 1993, pp. 73–78.

[11]Parr, T. P., Gutmark, E., Hanson-Parr, D. M., and Schadow, K. C., "Feedback Control of an Unstable Ducted Flame," *Journal of Propulsion and Power*, Vol. 9, No. 4, 1993, pp. 529–535.

[12]Padmanabhan, K. T., Bowman, C. T., and Powell, J. D., "An Adaptive Optimal Combustion Control Strategy," *Combustion and Flame*, Vol. 100, No. 1/2, 1995, pp. 101–110.

[13]Bloxsidge, G. J., Dowling, A. P., Hooper, N., and Langhorne, P. J., "Active Control of an Acoustically Driven Combustion Instability," *Journal of Theoretical and Applied Mechanics*, Special Issue, Supplement to Vol. 6, 1987, pp. 161–175.

[14]Langhorne, P. J., Dowling, A. P., and Hooper, N., "Practical Active Control System for Combustion Oscillations," *Journal of Propulsion and Power*, Vol. 6, No. 3, 1990, pp. 324–333.

[15]Billoud, G., Galland, M. A., Huynh Huu, C., and Candel, S., "Adaptive Active Control of Combustion Instabilities," *Combustion Science and Technology*, Vol. 81, No. 4–6, 1992, pp. 257–283.

[16]Schadow, K. C., Gutmark, E., and Wilson, K. J., "Active Combustion Control in a Coaxial Dump Combustor," *Combustion Science and Technology*, Vol. 81, No. 4–6, 1992, pp. 285–300.

[17]Culick, F. E. C., "Combustion Instabilities in Liquid-Fueled Propulsion Systems—An Overview," AGARD, CP-450, 1989, pp. 1–73.

[18]Candel, S. M., "Combustion Instabilities Coupled by Pressure Waves and Their Active Control," *Proceedings of the 24th Symposium (International) on Combustion*, Reinhold, New York, 1992, pp. 1277–1296.

[19]McManus, K. R., Poinsot, T., and Candel, S. M., "A Review of Active Control of Combustion Instabilities," *Progress in Energy and Combustion Science*, Vol. 19, No. 1, 1993, pp. 1–29.

[20]Koshigoe, S., Gillis, J. T., and Falangas, E. T., "A New Approach for Active Control of Sound Transmission Through an Elastic Plate Backed by a Rectangular Cavity," *Journal of the Acoustical Society of America*, Vol. 94, No. 2, 1993, pp. 900–907.

[21]Koshigoe, S., Teagle, A., and Gordon, A., "A Time Domain Study of Active Control of Sound Transmission Due to Acoustic Pulse Excitation," *Journal of the Acoustical Society of America*, Vol. 97, No. 1, 1995, pp. 313–323.

[22]Culick, F. E. C., and Yang, V., "Prediction of the Stability of Unsteady Motions in Solid-Propellant Rocket Motors," *Unsteady Burning and Combustion Stability of Solid Propellants*, edited by L. DeLuca, E. W. Price, and M. Summerfield, Vol. 143, Progress in Astronautics and Aeronautics, AIAA, Washington, DC, 1992, pp. 719–779.

[23]Crocco, L., and Cheng, S. I., *Theory of Combustion Instabilities in Liquid-Propellant Rocket Motors*, AGARDOGRAPH No. 8, Butterworths, London, 1956.

[24]Widrow, B., and Stearns, S. D., *Adaptive Signal Processing*, Prentice–Hall, Inc., Upper Saddle River, NJ, 1985, pp. 99–116.